Voltage-sensitive dye imaging of transcranial magnetic stimulation-induced intracortical dynamics

Vladislav Kozyrev[a], Ulf T. Eysel[b], and Dirk Jancke[a,1]

[a]Optical Imaging Group, Institut für Neuroinformatik, and [b]Department of Neurophysiology, Ruhr University Bochum, 44780 Bochum, Germany

Edited by Riitta Hari, School of Science, Aalto University, Espoo, Finland, and approved August 11, 2014 (received for review March 24, 2014)

Transcranial magnetic stimulation (TMS) is widely used in clinical interventions and basic neuroscience. Additionally, it has become a powerful tool to drive plastic changes in neuronal networks. However, highly resolved recordings of the immediate TMS effects have remained scarce, because existing recording techniques are limited in spatial or temporal resolution or are interfered with by the strong TMS-induced electric field. To circumvent these constraints, we performed optical imaging with voltage-sensitive dye (VSD) in an animal experimental setting using anaesthetized cats. The dye signals reflect gradual changes in the cells' membrane potential across several square millimeters of cortical tissue, thus enabling direct visualization of TMS-induced neuronal population dynamics. After application of a single TMS pulse across visual cortex, brief focal activation was immediately followed by synchronous suppression of a large pool of neurons. With consecutive magnetic pulses (10 Hz), widespread activity within this "basin of suppression" increased stepwise to suprathreshold levels and spontaneous activity was enhanced. Visual stimulation after repetitive TMS revealed long-term potentiation of evoked activity. Furthermore, loss of the "deceleration–acceleration" notch during the rising phase of the response, as a signature of fast intracortical inhibition detectable with VSD imaging, indicated weakened inhibition as an important driving force of increasing cortical excitability. In summary, our data show that high-frequency TMS changes the balance between excitation and inhibition in favor of an excitatory cortical state. VSD imaging may thus be a promising technique to trace TMS-induced changes in excitability and resulting plastic processes across cortical maps with high spatial and temporal resolutions.

excitation–inhibition balance | plasticity | primary visual cortex

Over recent decades, transcranial magnetic stimulation (1) (TMS) has become a frequently used method for noninvasive diagnostics, therapeutic treatment, and intervention for neurorehabilitation of neurological disorders (2–8). Additionally, TMS has proved a valuable tool in basic brain research as its perturbative effects allow area-selective manipulation of immediate cortical function (9–11), as well as its long-lasting alteration through plasticity and learning protocols (12, 13). However, direct measurements of the TMS-induced cortical dynamics at highly resolved spatiotemporal scales are missing because "online approaches" (14), using modern neuroimaging techniques such as functional MRI (fMRI) (15–18), magnetoencephalography (19), EEG (20), and near-infrared (21) or intrinsic optical imaging (22), are limited in either spatial or temporal resolutions or in both.

Here we overcame these limitations, using optical imaging with voltage-sensitive dyes (VSD), which exploits the dye's property to transduce gradual changes in voltage across neuronal membranes into fluorescent light signals. In contrast to imaging methods applicable in humans, this method is invasive but allows avoiding the commonly experienced contamination of signals by artifacts due to the strong TMS-induced electric field. In combination with a tandem-lens system of large numerical aperture (23) and a fast CCD camera as detector, VSD imaging captures several square millimeters of cortex with an emphasis on superficial layers (24–32), allowing us to record activity changes within milliseconds across millions of neurons at once with a spatial resolution of ∼50 μm (for review see ref. 33). We measured activity in cat primary visual cortex (V1) upon repetitive TMS (rTMS) (0.15 Hz, 1 Hz, and 10 Hz) and describe its effects on fundamental processing characteristics during subsequent visual stimulation.

Results

Space–Time Visualization of TMS-Induced Cortical Dynamics. VSD imaging enabled artifact-free visualization of TMS-induced activity across ∼7 × 3 mm of cortex depicted in Fig. 1 within 10-ms frames (Movie S1). A single TMS pulse (Fig. 1*C*, *Left* trace) led to brief focal activation with highest amplitudes closest to the coil (Fig. 1*C*, reddish area, first two frames after TMS onset) succeeded by immediate suppression (bluish colors). The decrease in activity lasted up to ∼300 ms followed by rebound activation that remained locally, surrounded by a suppressed area. These results demonstrate that after a 20-ms period of excitation following a single TMS pulse, the postsynaptic potentials of a large pool of neurons start nearly instantaneously and drastically, decreasing below baseline activity.

Applying high-frequency rTMS (10 Hz) (34, 35), we observed similar early phase suppression after the first pulse as expected (Fig. 1*C*, *Right* trace; Fig. 1*D* shows time courses of spatially averaged activities). However, in contrast to a single pulse, each further pulse triggered a consecutive boost in activity, building up to widespread activation levels. Note that the first pulse suppression in the 10-Hz condition appears smaller than for the

Significance

Transcranial magnetic stimulation (TMS) is significant for medical diagnostics, therapeutic treatment, and basic brain research. However, highly resolved observations of its immediate effects remained obscured because existing techniques are limited in spatial or temporal resolutions and are severely disturbed by the high magnetic fields. Here, we avoid these limitations, using optical imaging with voltage-sensitive dye (VSD) in the cat animal model. VSD transforms changes in neuronal membrane voltage into optical signals, providing microsecond resolution and evading contamination by electromagnetic artifacts. We visualize TMS-induced cortical dynamics and characterize effects on visual processing over scales of milliseconds, minutes, and hours. Combined TMS and VSD imaging offers a powerful approach to study targeted modifications in cortical function during TMS-based plasticity and learning protocols.

Author contributions: V.K., U.T.E., and D.J. designed research; V.K. and D.J. performed research; V.K. and D.J. analyzed data; V.K. and D.J. contributed new reagents/analytic tools; and D.J. wrote the paper, with input from all the authors.

The authors declare no conflict of interest.

This article is a PNAS Direct Submission.

Freely available online through the PNAS open access option.

[1]To whom correspondence should be addressed. Email: dirk.jancke@rub.de.

This article contains supporting information online at www.pnas.org/lookup/suppl/doi:10.1073/pnas.1405508111/-/DCSupplemental.

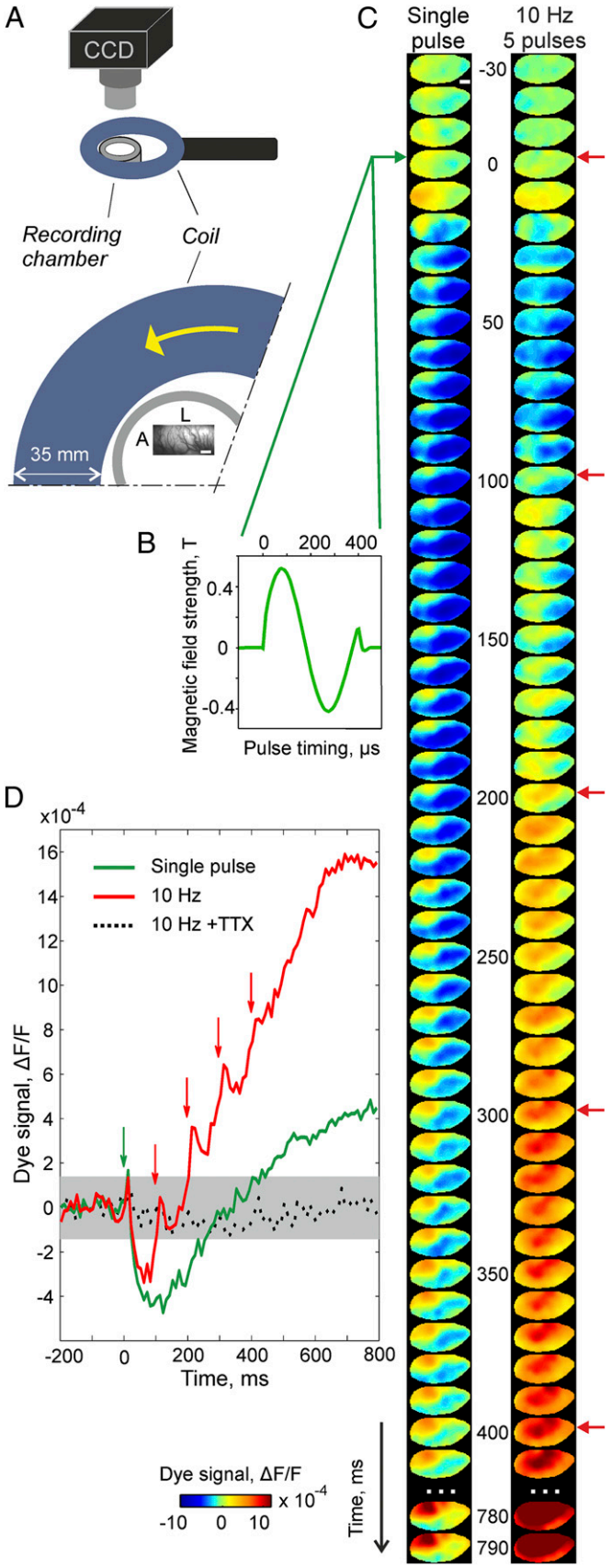

Fig. 1. Visualization of TMS-induced cortical activity using VSD imaging in a single experimental session. (*A*) Sketch of relative coil position (35-mm coil casing, blue), recording chamber (border outlined in gray, outer/inner diameter = 32/24 mm), and vascular pattern of the imaged region (cat V1, A, anterior; L , lateral). (Scale bar, 1 mm.) (*Lower*) Zoom in from *Upper*: The coil center was 9 mm medial and 8 mm posterior with respect to the center of the recording chamber (*Materials and Methods*). Yellow arrow indicates the first hemicycle current direction of the biphasic pulse. Measurements of cortical activity were achieved through metal-free optical and stereotactic settings (*Materials and Methods*). (*B*) Magnetic field strength and its timing measured separately in air (*Materials and Methods* shows estimates of induced electric field). (*C*) Spatiotemporal activity patterns induced by a single TMS pulse (*Left* trace) and 10 Hz TMS (*Right* trace, five pulses); green and red arrows mark time of stimulation. Activity was averaged over 40 repetitions. Colorbar indicates activity levels expressed as fractional change in fluorescence relative to blank condition ($\Delta F/F$). (*D*) Time courses of spatial averages across recording frames. Stippled black trace was recorded after application of TTX (10 Hz, 30 repetitions) to verify that no artifacts were present. Gray area depicts confidence levels (95%) of baseline activity. Ten hertz rTMS produced gradual buildup of activity after initial suppression present in both TMS conditions (green arrow overlaps first red).

low-frequency protocol. This is because averaging across multiple repetitions of TMS trials inevitably includes activity that was already enhanced through previous high-frequency trains, including persistently rising baseline activity (compare Fig. 2*C*) and possibly reduced effectiveness of inhibition. Thus, repetitive TMS pulses successively increased the overall postsynaptic potential levels from below baseline up to high amplitudes (crossing baseline after the third TMS pulse), suggesting a joint excitatory state across large neuronal populations.

These results were remarkably consistent across experiments (Fig. 2). In Fig. 2*A*, we depict spatially averaged activities in response to both single-pulse and 10-Hz TMS conditions as a mean across nine different cat experiments. Generally, the first TMS pulse led to brief excitation followed by immediate suppression (with duration of 250 ms ± 40 SD), similar to that observed earlier with extracellular electrode recordings using suprathreshold 1-Hz TMS (36). Levels of rebound activity after repetitive single-pulse TMS remained at low values (1.3 ± 0.9 SEM, $\times 10^{-4}$ $\Delta F/F$), whereas the stepwise increase in activity after 10 Hz rTMS produced significantly higher amplitudes (5.6 ± 1.6 SEM, $\times 10^{-4}$ $\Delta F/F$). Interestingly, when calculated from the suppressive baseline, net amplitudes induced by the 10-Hz rTMS trains after the last fifth pulse, denoted here as the late response phase (gray shaded in Fig. 2), were in the same range (9.0 ± 1.7 SEM, $\times 10^{4}$ $\Delta F/F$) as for visually evoked activity (8.3 ± 1.1 SEM, $\times 10^{-4}$ $\Delta F/F$, Fig. 2*B*). Visual activity was evoked with high-contrast full-field moving gratings as the most effective stimulus to drive spiking activity in V1 and used here as a standard control for maximal visual stimulation. Furthermore, the threshold for the emergence of average spiking activity of neural populations was recently approximated with 30–40% of the maximal visually evoked VSD imaging signals (37). Hence, it is most likely that 10 Hz rTMS induced extensive spiking population activity, especially during the late response phase after stimulation.

Excitatory Cortical State After 10 Hz rTMS. We next determined how the rTMS-induced changes in cortical excitation levels were reflected in ongoing, i.e., spontaneous, activity. For this purpose, we made use of our stimulation protocol where we measured repeated blocks of two blank trials, during which spontaneous activity was recorded, followed by five trials of 10-Hz trains (five pulses within each trial) and another final blank condition. The time interval between trials was 7 s. Hence, the third blank was measured 35 s after the first TMS pulse in each block. Within blocks, each lasting ∼1 min, we found a consecutive enhancement of activity up to the last blank (Fig. S1) (ref. 22 shows similar observations of TMS-enhanced spontaneous activity). Fig. 2*C* depicts activity within the latter blank averaged over 8–12

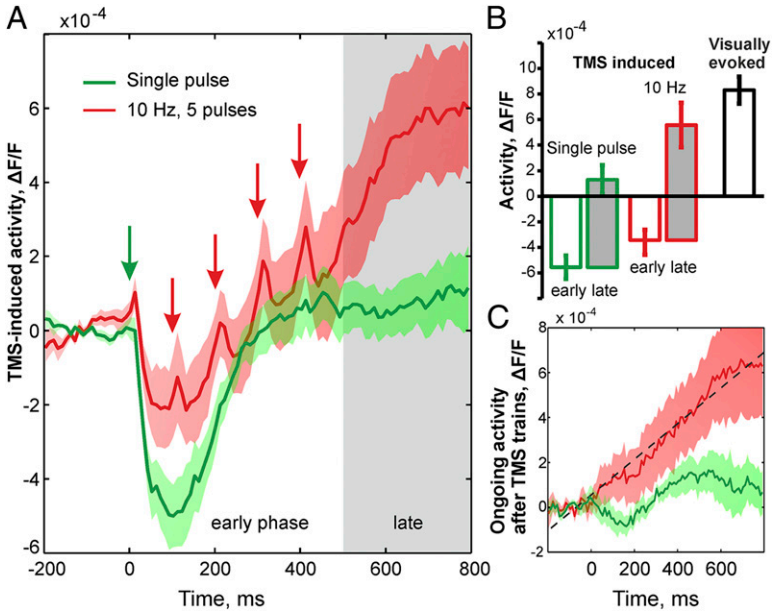

Fig. 2. Buildup of an excitatory cortical state through high-frequency rTMS (nine different experiments). (*A*) Initial TMS pulses induced strong suppression followed by rebound of small amplitude in the case of single-pulse stimulation (green). Contrastingly, in the case of 10 Hz (red) each consecutive TMS pulse gave rise to a stepwise increase in cortical activity. Arrows mark TMS pulse time (first red arrow is covered by the green). Color shadings depict SEM. When calculated from the suppressive baseline, amplitudes of activity following 10 Hz TMS were in the same range (right bar in *B*) and highly correlated with visually evoked responses ($r = 0.81$, pairwise comparisons). Note that for low-frequency stimulation, the first-pulse excitatory peak appeared less pronounced than that for 10 Hz, because its onset was scattered across experiments, possibly reflecting reduced excitability. (*B*) TMS-induced amplitudes of activity during early phase (white bar, mean across five time frames with lowest responses) and late phase (gray bar, mean between 500 ms and 800 ms; compare gray area in *A*) compared with visually evoked responses (black contour). Error bars depict SEM. (*C*) Spontaneous activity after 10 Hz rTMS (red) revealed monotonous increase (8×10^{-4} units/s, dashed line shows linear regression) not present after low-frequency stimulation (green).

block repetitions across experiments. The evolution of activity, using the first two blanks as a reference, showed a monotonous increase (Fig. 2*C*, red curve). Thus, starting from a common baseline, ongoing activity underwent a persistent rise, suggesting an underlying excitatory cortical state emerging within 8–12 min in the case of 10 Hz rTMS but not for single-pulse stimulation (Fig. 2*C*, green curve).

Effects on Visual Cortical Processing—Long-Term Potentiation– and Long-Term Depression–Like Activation and Suppression. How does the excitatory state induced by application of 10 Hz rTMS influence visual cortical excitability? In cat V1, 1 Hz rTMS was shown to reduce visually evoked potentials whereas 10 Hz rTMS led to increased amplitudes (35). Likewise in human visual cortex, 1 Hz vs. 10 Hz TMS regimes showed opposing effects on excitability, as measured by changes of phosphene thresholds (38, 39). In particular, effectiveness of 10 Hz rTMS over human V1 was demonstrated by improved contrast sensitivity of amblyopic patients (40), as well as by modulation of performance in visual detection and feature discrimination tasks (41).

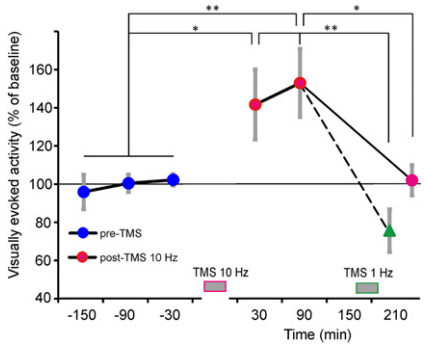

Fig. 3. Induction of LTP-like facilitation. After application of 10 Hz rTMS (red data points), visually evoked activity was enhanced for 30–90 min ($n = 13$ experiments) compared with pre-TMS times (blue). This effect was counteracted by subsequent application of 1 Hz TMS, resulting in LTD-like suppression (green, $n = 4$), but also declined to baseline levels without further interventions ($n = 5$). Gray bars at bottom mark TMS times; $^*P < 0.05$, $^{**}P < 0.01$, two-sample two-tailed *t* test; vertical gray lines show SEM.

We imaged visually evoked activity, presenting high-contrast gratings before and after 25–30 min of 10 Hz rTMS (*Materials and Methods*). Visually evoked responses measured 30–90 min after rTMS were increased up to 53% in comparison with baseline values (Fig. 3). This effect lasted for 2–3 h, suggesting "early" long-term potentiation (LTP) (42), and returned to baseline after 3–4 h without further intervention. Interestingly, LTP-like activation could directly be turned into long-term depression (LTD) by subsequent application of 1 Hz rTMS (Fig. 3, green triangle). Hence, in summary we demonstrate facilitatory visual effects upon 10 Hz TMS (34, 35) and suggest LTP/LTD-like plastic changes in synaptic efficacy dependent on TMS stimulation frequency (reviews in refs. 43–45).

rTMS Decreases Impact of Intracortical Inhibition. Despite its wide application, the impact of TMS on cortical processing is poorly understood in terms of the affected neuronal network mechanisms. We here make use of the unique property of VSD imaging to allow observing the gradual changes in synaptic activity at the population level. Specifically during the rise time of visually evoked activity, VSD imaging is capable of detecting a notch attributed to intracortical inhibition counteracting the excitatory input drive (24, 46). Importantly, this so-called deceleration–acceleration ("DA") notch was shown to reflect cross-orientation inhibition (46–48) contributing to sharpened orientation tuning and thus demonstrating its functional relevance for intracortical processing (blue curves in Fig. 4 *A–E* show typical examples).

Strikingly, after application of 10 Hz rTMS the notch was diminished, indicating weakened inhibition (Fig. 4, pink curves). Fig. 4*G* graphs summarize the disappearance of the notch after rTMS and the increase in evoked amplitudes across nine different experiments, notably without normalization or alignment of the individual time courses, emphasizing the consistency of the obtained results. The pre/post-TMS difference in visually driven time courses started at ~65 ms after stimulus onset (asterisk in Fig. 4*G*, $P < 0.05$, two-tailed *t* test) and persisted until the end of the trial. As a consequence, activity reached higher amplitudes compared with pre-TMS levels (Fig. 4*G*, *Right* graphs). Importantly, in a 10-Hz sham control no changes in activity time courses were observed across the entire experimental duration (Fig. S2).

Finally, to further control whether diminishing of the notch was merely related to unspecific weakening of inhibition over the time course of the experiments, we applied 1 Hz rTMS after the 10 Hz rTMS plasticity protocol. We found that the notch

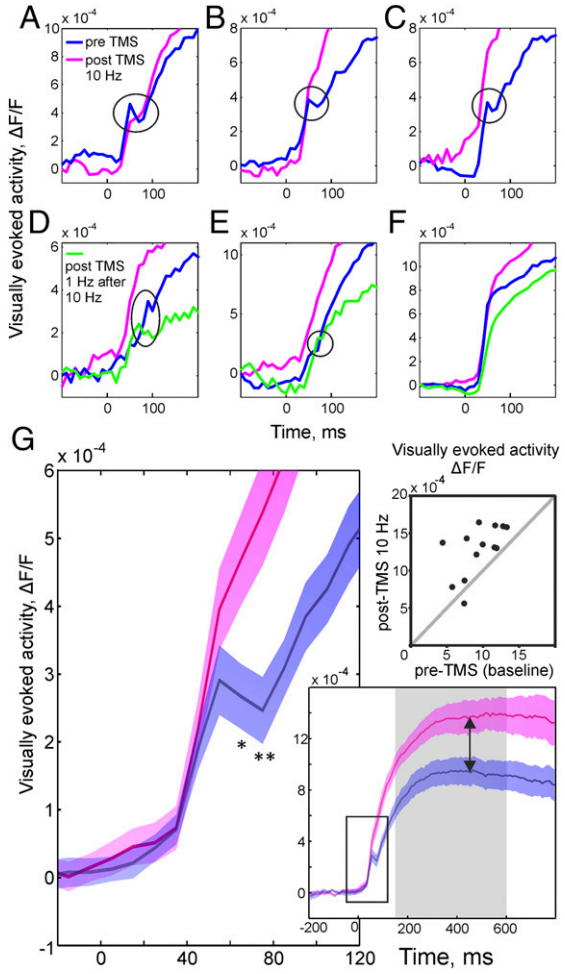

Fig. 4. Weakened inhibition after high-frequency rTMS. Traces depict evolution of visually evoked activity over time (spatial averages across image frames). Before application of TMS, a notch during the rising phase (blue curves) was evident, indicating inhibition (main text). In *A–E*, individual experiments are shown with the notch encircled. After 10 Hz rTMS notches were almost completely abolished (pink curves), suggesting weakened inhibition, leading to higher amplitudes and shorter response latencies (compare blue and pink curves). Controls with subsequent application of 1 Hz rTMS (*D* and *E*, green curves) showed reduction of response amplitudes and recurrence of the notch, signifying regained inhibition. In 4 of 13 experiments, the notch was absent from the start (example in *F*); the opposing effects of single-pulse vs. 10 Hz TMS on response amplitudes were, however, clearly present. (*G*, *Left*) Mean across 9 different experiments (colored areas show SEM). Pre-TMS (blue) activity during the notch phase was significantly lower (with maximal effect 75 ms after stimulus onset, $^{**}P < 0.01$, two-tailed *t* test) than after 10 Hz rTMS (pink). Amplitudes at 75 ms in pre-TMS conditions were on average 2.6 ± 0.4 SEM, $\times 10^{-4}$ $\Delta F/F$ compared with 5.4 ± 0.7 SEM, $\times 10^{-4}$ $\Delta F/F$ after rTMS. (*Lower Right*) Time courses between −200 ms and 800 ms, stimulus onset at zero. Arrows point to differences in amplitudes. Square outlines zoom-in shown at *Left*. (*Upper Right*) Pre- and post-TMS (10 Hz) differences in visually evoked amplitudes (time averages across the gray-shaded timespan in *Lower* plot) for the individual experiments ($n = 13$).

reappeared, demonstrating that inhibition was regained and ruling out unspecific effects on inhibitory drive after prolonged 10 Hz rTMS (Fig. 4 *D* and *E*). Still it might be possible that the applied combination of high- and low-frequency rTMS triggered additional homeostatic mechanisms, for example involving glutamatergic modulation of interneurons (49).

In summary our data suggest that the immediate effect of repetitive TMS pulses is to weaken intracortical inhibition. Reduced inhibition might thus be an initial driving force for early LTP effects and increased cortical excitability after high-frequency rTMS.

Discussion

Using VSD in an "on-line TMS-neuroimaging approach" (14), we provide for the first time to our knowledge highly resolved spatiotemporal data of TMS-induced cortical dynamics at the population level. In particular, we show artifact-free measurements of local intracortical events within the immediate 10 ms following a given TMS pulse.

Whereas VSD imaging is limited to animal models because of its invasive nature, other imaging methods such as EEG or fMRI allow human applications. In contrast to imaging of blood oxygen level-dependent (BOLD) signals, which are inevitably slow because of their dependence on hemodynamics, we here measured neuronal activity directly as voltage changes across neuronal membranes. Commonly, immediate detection of the fluctuations in neuronal membrane potentials suffers from artifacts introduced by the TMS coil discharge, leading to overload of recording amplifiers around the time point of TMS pulses (22, 36) and masking of neuronal effects, which can gradually be reduced by only advanced technologies (50–53). Obviously, VSD imaging does not provide single-cell resolution and is limited to cortical surface areas. On the other hand, it avoids biased sampling of neurons and also captures their subthreshold responses (25, 27, 54), hence providing a global picture of the net activation levels across neuronal populations under different stimulus conditions. As the VSD acts as a molecular transducer by transforming voltage into optical signals, our method provides as such microsecond time resolution and additionally avoids the above-mentioned electricity-dependent artifact problems.

We showed over a milliseconds to several minutes timescale that, following a first single TMS magnetic pulse, cortical population activity briefly peaks and then immediately declines much below baseline, indicating suppression. This suggests that TMS delivers a strong volley that predominantly affects inhibitory neurons (55, 56), most likely of the parvalbumin-expressing type (57). Because of their soma targeting on pyramidal neurons (58), and possibly because of their far-reaching axonal-dendritic structure (59) enhancing TMS sensitivity (60), these interneurons may impose strong synchronized inhibition in the affected cortical network (10).

To provide evidence that the observed suppression most likely does not reflect overriding intrinsic signals (e.g., hemodynamic related changes due to vessel constriction, light scatter changes) and depends on the functional state of the cortex, we combined a single TMS pulse with simultaneous visual stimulation (Fig. S3). By temporally resolving cortical responses to each TMS pulse, we demonstrate that starting from the initial "basin of suppression," consecutive TMS pulses (10 Hz) produce a stepwise buildup of activity, reaching signal levels that suggest massive spiking across large populations of neurons. These results promote the view that subsequent TMS pulses, each within a 100-ms time window, weaken inhibitory drive (57) and activate excitatory circuits that outbalance inhibition involving NMDA-receptor activation (61), overall leading to an excitatory state of the cortex (62).

We then investigated how continuous rTMS (20–30 min) affects visual processing. First, we showed opposing effects of TMS frequency in that 1 Hz stimulation led to LTD whereas 10 Hz rTMS led to LTP-like behavior, evident in lower and higher amplitudes of evoked visual responses, respectively. Similar effects of increased or decreased excitability dependent on TMS frequency were originally found in motor cortex (63, 64). Second, we addressed the question of how early LTP, along with the observed increase in excitability, influences cortical activation dynamics. In fact, there is a considerable uncertainty about the neuronal mechanisms underlying plastic TMS effects, particularly

regarding LTP-like functioning (45, 65). We found that the DA notch (46), as a signature of intracortical inhibition counteracting the excitatory visual input during the rising phase of cortical responses (24), was diminished (reversible through low-frequency TMS). The disappearance of the notch does not exclude additional involvement of facilitatory mechanisms acting on longer timescales (42) and changing excitation–inhibition balance in favor of LTP-like excitation. Additionally, volatile anesthesia as used here reduces spontaneous activity and increases inhibition (66). Hence, the excitatory levels found after high-frequency stimulation might be underestimated, whereas notch strength before TMS might be overestimated. Future studies may provide further mechanistic insights through systematic variation in TMS intensity (35, 67, 68) or by testing the dependence of the TMS effect on cortical states (22, 39, 49, 69). However, our results suggest reduced inhibitory drive as one major origin of rTMS-induced increased excitability of the visual cortex.

In conclusion, we have shown that combining TMS with VSD imaging allows highly resolved visualization of TMS-induced population dynamics—both at sub- and at suprathreshold synaptic levels—across several square millimeters of cortex in an animal model. In the future, these capacities might provide a powerful approach to study cortical reorganization processes (70, 71) of the functional neuronal architecture induced by TMS-based plasticity and learning protocols.

Materials and Methods

Preparation for Optical Imaging. All experiments were carried out in accordance with the European Union Community Council guidelines and approved by the German Animal Care and Use Committee (application no. AZ 87-51.04.2010.A305) in accordance with the Deutsches Tierschutzgesetz (section 8 Abs. 1) and the National Institutes of Health guidelines. We applied TMS and visual stimuli to cats ($n = 15$, 7 males and 8 females, adult). Animals were initially anesthetized with ketamine (20 mg·kg^{-1} i.m.) and xylazine (20 mg·mL^{-1}, 0.03 mL·kg^{-1} i.m.) and then continuously anesthetized and artificially respirated with 0.8–1.5% (vol/vol) isoflurane in a 1:2 mixture of O_2/N_2O, fed intravenously, and paralyzed after surgery by i.v. perfusion of Pancuronium (0.04–0.05 mg·kg^{-1}·h^{-1}; Inresa). We administered Fortecortin (0.4 mg·kg^{-1} i.m.; Merck) and atropine sulfate (0.05 mg·kg^{-1} i.m.) daily and perfused i.v. Cephazolin (2 mg·kg^{-1}·h^{-1}; Fresenius). Heart rate, intratracheal pressure, exhaled CO_2, and body temperature were monitored. To avoid artifacts due to eddy currents in nearby metal parts, the stereotaxic frame was constructed using polyoxymethylene (POM) as material. Additionally, the recording chamber was made of polyether ether ketone (PEEK). The chamber was mounted after the skull was opened above the visual cortex (area 18, occasionally including parts of area 17). The dura was removed and the cortex was stained for ∼3 h with voltage-sensitive dye (RH-1691). For further details see ref. 54.

Transcranial Magnetic Stimulation. Magnetic pulses were generated by a MagStim rapid^2 stimulator (The Magstim Company Ltd.) and applied to the occipital cortex via a 90-mm circular coil (to optimize camera access, 11 experiments) or a 70-mm figure-of-eight coil (4 experiments). Coils were covered with wet cotton compresses ventilated by a microventilator to avoid overheating. The circular coil was placed 5–10 mm above the skull enclosing the cranial chamber as shown schematically in Fig.1*A*. To position the strongest induced electric field as close as possible to the imaged area, and at the same time to avoid any contact with stereotactic equipment in front of the animal, the coil was placed slightly off center with respect to the recording chamber. When a double coil was used, it was positioned obliquely behind the cat's head closest to the chamber. In all cases coil position was adjusted to create an unobstructed view through the camera lens. Stimulator output was measured by a semiconductor probe based on n-type doped Ga-As heterostructure (A. Wieck, Faculty of Physics, Ruhr University Bochum). The stimulator generated 400-μs biphasic magnetic pulses, and output was set to 60% of maximal intensity, corresponding to peak magnetic field strength of 0.2–0.5 T (Fig. 1*B*) and induced electric field of 25–80 V·m^{-1} at the location of the imaged cortex (estimation procedure in *SI Text 1*). TMS-evoked peripheral muscle contractions before paralysis of the animal indicated stimulation strength above motor threshold.

Data Acquisition and Processing. Optical imaging was performed using Imager 3001 (Optical Imaging Inc.). As a crucial step, to avoid TMS-induced camera movement artifacts, we rebuilt the optics of an original 50-mm Nikon lens system within a chassis of plastic material (PEEK). The camera was focused ∼500 μm below the cortical surface. Data acquisition onset was synchronized with heartbeat and respiration. For detection of changes in fluorescence the cortex was illuminated with light of wavelength 630 ± 10 nm and emitted light above 665 nm was collected. The recording frame rate was set to 100 Hz. The raw imaging data were preprocessed by dividing each pixel value by an average 200 ms prestimulus activity and subsequently subtracted by the average of two blanks (i.e., recordings without TMS or visual stimulus, see below) to remove heartbeat and respiration noise. These processing steps led to a unitless relative signal of fluorescence changes, denoted by $\Delta F/F$.

TMS Protocols. ***Combined TMS and VSD imaging.*** Each recording block comprised two blank trials, where spontaneous activity was recorded, followed by five trials of either 0.15 Hz (referred to as "single TMS pulses") or 10 Hz TMS (five pulses within each trial) and a final blank trial. Each trial spanned 1 s, including 200 ms prestimulus time.

Plasticity protocol. To affect cortical excitability and plasticity, TMS was applied for a period of 25–30 min. The protocols contained sequences of five pulses (10 Hz) triggered every 7 s, corresponding to the TMS protocols used during combined VSD imaging (see above), or low-frequency sequences (1 Hz, 2 × 600 pulses, separated by 10 min to avoid overheating of the coil), while coil positioning and TMS intensity were kept constant over the entire experiment.

Visual Stimuli. To measure visually evoked cortical responses, moving sine-wave gratings were used (Michelson's contrast: 1 and 0.2 cycles per degree, 6 cycles per second, mean luminance 35 cd/m^2) with eight orientations (22.5° steps, seven experiments) or two to four orthogonal orientations (eight experiments), including opposite motion directions. For analysis, activity across all orientations was averaged. Additionally, two blank conditions were recorded, in which an isoluminant gray screen was shown. Trials were presented in pseudorandom order, and each trial lasted 1 s, including 200 ms prestimulus time. VSD imaging of evoked responses was carried out for 2–4 h before and after the TMS plasticity protocol to follow the time course of alterations of cortical function due to TMS.

Analysis of TMS-Induced Activity. Experimental datasets comprised at least 30 repetitions of trials with either visual or magnetic stimulation. This trial number provided normal distributions of the observed activation values (Lilliefors test at 5% significance level) and allowed using parametric statistics in most of the cases. The region of interest (ROI) was set by encircling the area of the image in which clear visual responses were observed. Images were corrected by the SD of the first blank condition (formulas in *SI Text 2*).

Tetrodotoxin Citrate. To control for contamination of the imaging signals by possible vibrational artifacts during TMS, we used tetrodotoxin citrate (TTX) (Tocris Bioscience) to selectively block sodium channels and to thus inactivate the recorded cortical tissue ($n = 9$ different experiments; example in Fig. 1*D*, stippled line). The chamber was filled with 20 μM TTX dissolved in Ringer's solution for 30 min. Application of TTX abolished both the visual and the TMS-induced activation without indication of artifacts in all experiments where the custom-built PEEK camera lens was used.

ACKNOWLEDGMENTS. We thank Dr. Andreas Wieck for the custom-made semiconductor probe and valuable technical advice; Tobias Grunewald for magnetic field measurements; Stefan Dobers and Hans-Dieter Knoop (mechanical shop of Faculty of Biology and Biotechnology, Ruhr-University Bochum) for excellent technical assistance; Christian Vilter, Clemens Wirtz, and Holger Zemzycki (mechanical shop of the Faculty of Physics and Astronomy, Ruhr-University Bochum) for in-house PEEK rebuild of a Nikon lens chassis; and Sascha Rekauzke for assistance during experiments. We thank Drs. Hubert Dinse and Klaus Funke for helpful discussions on the manuscript. This work was financially supported by the Deutsche Forschungsgemeinschaft (DFG) (SFB 874 TP A2 to D.J. and U.T.E.), the German–Israeli Project Cooperation (JA 945/3-1), and the DFG priority programme 1665 (JA 945/4-1).

1. Barker AT, Jalinous R, Freeston IL (1985) Non-invasive magnetic stimulation of human motor cortex. *Lancet* 1(8437):1106–1107.
2. Lefaucheur JP, Drouot X, Keravel Y, Nguyen JP (2001) Pain relief induced by repetitive transcranial magnetic stimulation of precentral cortex. *Neuroreport* 12(13):2963–2965.
3. Hamer HM, et al. (2005) Motor cortex excitability in focal epilepsies not including the primary motor area—a TMS study. *Brain* 128(Pt 4):811–818.
4. Kleinjung T, et al. (2005) Long-term effects of repetitive transcranial magnetic stimulation (rTMS) in patients with chronic tinnitus. *Otolaryngol Head Neck Surg* 132(4):566–569.

5. Höflich G, Kasper S, Hufnagel A, Ruhrmann S, Möller H-J (1993) Application of transcranial magnetic stimulation in treatment of drug-resistant major depression - a report of 2 cases. *Hum Psychopharmacol* 8:361–363.
6. Loo CK, Mitchell PB (2005) A review of the efficacy of transcranial magnetic stimulation (TMS) treatment for depression, and current and future strategies to optimize efficacy. *J Affect Disord* 88(3):255–267.
7. Hummel F, Cohen LG (2005) Improvement of motor function with noninvasive cortical stimulation in a patient with chronic stroke. *Neurorehabil Neural Repair* 19(1):14–19.
8. McKinley RA, Bridges N, Walters CM, Nelson J (2012) Modulating the brain at work using noninvasive transcranial stimulation. *Neuroimage* 59(1):129–137.
9. Jahanshahi M, Dirnberger G (1999) The left dorsolateral prefrontal cortex and random generation of responses: Studies with transcranial magnetic stimulation. *Neuropsychologia* 37(2):181–190.
10. Pascual-Leone A, Walsh V, Rothwell J (2000) Transcranial magnetic stimulation in cognitive neuroscience—virtual lesion, chronometry, and functional connectivity. *Curr Opin Neurobiol* 10(2):232–237.
11. Walsh V, Cowey A (2000) Transcranial magnetic stimulation and cognitive neuroscience. *Nat Rev Neurosci* 1(1):73–79.
12. Tegenthoff M, et al. (2005) Improvement of tactile discrimination performance and enlargement of cortical somatosensory maps after 5 Hz rTMS. *PLoS Biol* 3(11):e362.
13. Waterston ML, Pack CC (2010) Improved discrimination of visual stimuli following repetitive transcranial magnetic stimulation. *PLoS ONE* 5(4):e10354.
14. Siebner HR, et al. (2009) Consensus paper: Combining transcranial stimulation with neuroimaging. *Brain Stimulat* 2(2):58–80.
15. Bohning DE, et al. (1997) Mapping transcranial magnetic stimulation (TMS) fields in vivo with MRI. *Neuroreport* 8(11):2535–2538.
16. Paus T, et al. (1997) Transcranial magnetic stimulation during positron emission tomography: A new method for studying connectivity of the human cerebral cortex. *J Neurosci* 17(9):3178–3184.
17. Roberts DR, et al. (1997) Multi-modality mapping of motor cortex: Comparing echoplanar BOLD fMRI and transcranial magnetic stimulation. Short communication. *J Neural Transm* 104(8–9):833–843.
18. Bestmann S, et al. (2008) Mapping causal interregional influences with concurrent TMS-fMRI. *Exp Brain Res* 191(4):383–402.
19. Kähkönen S, Marttinen Rossi E, Yamashita H (2005) Alcohol impairs auditory processing of frequency changes and novel sounds: A combined MEG and EEG study. *Psychopharmacology* 177(4):366–372.
20. Ilmoniemi RJ, et al. (1997) Neuronal responses to magnetic stimulation reveal cortical reactivity and connectivity. *Neuroreport* 8(16):3537–3540.
21. Parks NA, et al. (2012) Examining cortical dynamics and connectivity with simultaneous single-pulse transcranial magnetic stimulation and fast optical imaging. *Neuroimage* 59(3):2504–2510.
22. Allen EA, Pasley BN, Duong T, Freeman RD (2007) Transcranial magnetic stimulation elicits coupled neural and hemodynamic consequences. *Science* 317(5846):1918–1921.
23. Ratzlaff EH, Grinvald A (1991) A tandem-lens epifluorescence macroscope: Hundred-fold brightness advantage for wide-field imaging. *J Neurosci Methods* 36(2–3): 127–137.
24. Onat S, König P, Jancke D (2011) Natural scene evoked population dynamics across cat primary visual cortex captured with voltage-sensitive dye imaging. *Cereb Cortex* 21(11):2542–2554.
25. Grinvald A, Lieke EE, Frostig RD, Hildesheim R (1994) Cortical point-spread function and long-range lateral interactions revealed by real-time optical imaging of macaque monkey primary visual cortex. *J Neurosci* 14(5 Pt 1):2545–2568.
26. Petersen CC, Grinvald A, Sakmann B (2003) Spatiotemporal dynamics of sensory responses in layer 2/3 of rat barrel cortex measured in vivo by voltage-sensitive dye imaging combined with whole-cell voltage recordings and neuron reconstructions. *J Neurosci* 23(4):1298–1309.
27. Jancke D, Chavane F, Naaman S, Grinvald A (2004) Imaging cortical correlates of illusion in early visual cortex. *Nature* 428(6981):423–426.
28. Chen Y, Geisler WS, Seidemann E (2006) Optimal decoding of correlated neural population responses in the primate visual cortex. *Nat Neurosci* 9(11):1412–1420.
29. Roland PE, et al. (2006) Cortical feedback depolarization waves: A mechanism of top-down influence on early visual areas. *Proc Natl Acad Sci USA* 103(33):12586–12591.
30. Sit YF, Chen Y, Geisler WS, Miikkulainen R, Seidemann E (2009) Complex dynamics of V1 population responses explained by a simple gain-control model. *Neuron* 64(6): 943–956.
31. Berger T, et al. (2007) Combined voltage and calcium epifluorescence imaging in vitro and in vivo reveals subthreshold and suprathreshold dynamics of mouse barrel cortex. *J Neurophysiol* 97(5):3751–3762.
32. Onat S, Nortmann N, Rekauzke S, König P, Jancke D (2011) Independent encoding of grating motion across stationary feature maps in primary visual cortex visualized with voltage-sensitive dye imaging. *Neuroimage* 55(4):1763–1770.
33. Grinvald A, Hildesheim R (2004) VSDI: A new era in functional imaging of cortical dynamics. *Nat Rev Neurosci* 5(11):874–885.
34. Bohotin V, et al. (2002) Effects of repetitive transcranial magnetic stimulation on visual evoked potentials in migraine. *Brain* 125(Pt 4):912–922.
35. Aydin-Abidin S, Moliadze V, Eysel UT, Funke K (2006) Effects of repetitive TMS on visually evoked potentials and EEG in the anaesthetized cat: Dependence on stimulus frequency and train duration. *J Physiol* 574(Pt 2):443–455.
36. Moliadze V, Zhao Y, Eysel U, Funke K (2003) Effect of transcranial magnetic stimulation on single-unit activity in the cat primary visual cortex. *J Physiol* 553(Pt 2): 665–679.
37. Chen Y, Palmer CR, Seidemann E (2012) The relationship between voltage-sensitive dye imaging signals and spiking activity of neural populations in primate V1. *J Neurophysiol* 107(12):3281–3295.
38. Boroojerdi B, Prager A, Muellbacher W, Cohen LG (2000) Reduction of human visual cortex excitability using 1-Hz transcranial magnetic stimulation. *Neurology* 54(7): 1529–1531.
39. Fierro B, et al. (2005) Modulatory effects of low- and high-frequency repetitive transcranial magnetic stimulation on visual cortex of healthy subjects undergoing light deprivation. *J Physiol* 565(Pt 2):659–665.
40. Thompson B, Mansouri B, Koski L, Hess RF (2008) Brain plasticity in the adult: Modulation of function in amblyopia with rTMS. *Curr Biol* 18(14):1067–1071.
41. Romei V, Gross J, Thut G (2010) On the role of prestimulus alpha rhythms over occipito-parietal areas in visual input regulation: Correlation or causation? *J Neurosci* 30(25):8692–8697.
42. Frey U, Morris RG (1998) Weak before strong: Dissociating synaptic tagging and plasticity-factor accounts of late-LTP. *Neuropharmacology* 37(4–5):545–552.
43. Hallett M (2007) Transcranial magnetic stimulation: a primer. *Neuron* 55(2):187–199.
44. Ridding MC, Rothwell JC (2007) Is there a future for therapeutic use of transcranial magnetic stimulation? *Nat Rev Neurosci* 8(7):559–567.
45. Hoogendam JM, Ramakers GM, Di Lazzaro V (2010) Physiology of repetitive transcranial magnetic stimulation of the human brain. *Brain Stimulat* 3(2):95–118.
46. Sharon D, Grinvald A (2002) Dynamics and constancy in cortical spatiotemporal patterns of orientation processing. *Science* 295(5554):512–515.
47. Sillito AM (1975) The contribution of inhibitory mechanisms to the receptive field properties of neurones in the striate cortex of the cat. *J Physiol* 250(2):305–329.
48. Morrone MC, Burr DC, Speed HD (1987) Cross-orientation inhibition in cat is GABA mediated. *Exp Brain Res* 67(3):635–644.
49. Barr MS, et al. (2011) The effect of repetitive transcranial magnetic stimulation on gamma oscillatory activity in schizophrenia. *PLoS ONE* 6(7):e22627.
50. Virtanen J, Ruohonen J, Näätänen R, Ilmoniemi RJ (1999) Instrumentation for the measurement of electric brain responses to transcranial magnetic stimulation. *Med Biol Eng Comput* 37(3):322–326.
51. Thut G, Ives JR, Kampmann F, Pastor MA, Pascual-Leone A (2005) A new device and protocol for combining TMS and online recordings of EEG and evoked potentials. *J Neurosci Methods* 141(2):207–217.
52. Bonato C, Miniussi C, Rossini PM (2006) Transcranial magnetic stimulation and cortical evoked potentials: A TMS/EEG co-registration study. *Clin Neurophysiol* 117(8): 1699–1707.
53. Daskalakis ZJ, Farzan F, Radhu N, Fitzgerald PB (2012) Combined transcranial magnetic stimulation and electroencephalography: Its past, present and future. *Brain Res* 1463(2):93–107.
54. Onat S, Jancke D, König P (2013) Cortical long-range interactions embed statistical knowledge of natural sensory input: A voltage-sensitive dye imaging study. *F1000 Res* 2:51.
55. Werhahn KJ, Kunesch E, Noachtar S, Benecke R, Classen J (1999) Differential effects on motorcortical inhibition induced by blockade of GABA uptake in humans. *J Physiol* 517(Pt 2):591–597.
56. Ziemann U (2003) Pharmacology of TMS. *Suppl Clin Neurophysiol* 56:226–231.
57. Benali A, et al. (2011) Theta-burst transcranial magnetic stimulation alters cortical inhibition. *J Neurosci* 31(4):1193–1203.
58. Markram H, et al. (2004) Interneurons of the neocortical inhibitory system. *Nat Rev Neurosci* 5(10):793–807.
59. Chung K, et al. (2013) Structural and molecular interrogation of intact biological systems. *Nature* 497(7449):332–337.
60. McAllister SM, Rothwell JC, Ridding MC (2009) Selective modulation of intracortical inhibition by low-intensity Theta Burst Stimulation. *Clin Neurophysiol* 120(4):820–826.
61. Huang YZ, Chen RS, Rothwell JC, Wen HY (2007) The after-effect of human theta burst stimulation is NMDA receptor dependent. *Clin Neurophysiol* 118(5):1028–1032.
62. Stagg CJ, et al. (2011) Relationship between physiological measures of excitability and levels of glutamate and GABA in the human motor cortex. *J Physiol* 589(Pt 23): 5845–5855.
63. Pascual-Leone A, Valls-Solé J, Wassermann EM, Hallett M (1994) Responses to rapid-rate transcranial magnetic stimulation of the human motor cortex. *Brain* 117(Pt 4): 847–858.
64. Chen R, et al. (1997) Depression of motor cortex excitability by low-frequency transcranial magnetic stimulation. *Neurology* 48(5):1398–1403.
65. Pell GS, Roth Y, Zangen A (2011) Modulation of cortical excitability induced by repetitive transcranial magnetic stimulation: Influence of timing and geometrical parameters and underlying mechanisms. *Prog Neurobiol* 93(1):59–98.
66. Hentschke H, Schwarz C, Antkowiak B (2005) Neocortex is the major target of sedative concentrations of volatile anaesthetics: Strong depression of firing rates and increase of GABAA receptor-mediated inhibition. *Eur J Neurosci* 21(1):93–102.
67. Ogiue-Ikeda M, Kawato S, Ueno S (2003) The effect of repetitive transcranial magnetic stimulation on long-term potentiation in rat hippocampus depends on stimulus intensity. *Brain Res* 993(1–2):222–226.
68. Bestmann S, Baudewig J, Siebner HR, Rothwell JC, Frahm J (2004) Functional MRI of the immediate impact of transcranial magnetic stimulation on cortical and subcortical motor circuits. *Eur J Neurosci* 19(7):1950–1962.
69. Silvanto J, Pascual-Leone A (2008) State-dependency of transcranial magnetic stimulation. *Brain Topogr* 21(1):1–10.
70. Das A, Gilbert CD (1995) Long-range horizontal connections and their role in cortical reorganization revealed by optical recording of cat primary visual cortex. *Nature* 375(6534):780–784.
71. Palagina G, Eysel UT, Jancke D (2009) Strengthening of lateral activation in adult rat visual cortex after retinal lesions captured with voltage-sensitive dye imaging in vivo. *Proc Natl Acad Sci USA* 106(21):8743–8747.